

The spin Hall angle and spin diffusion length of Pd measured by spin pumping and microwave photoresistance

Cite as: J. Appl. Phys. **115**, 17C504 (2014); <https://doi.org/10.1063/1.4862215>

Submitted: 22 September 2013 . Accepted: 17 October 2013 . Published Online: 16 January 2014

X. D. Tao, Z. Feng, B. F. Miao, L. Sun, B. You, D. Wu, J. Du, W. Zhang, and H. F. Ding



View Online



Export Citation



CrossMark

ARTICLES YOU MAY BE INTERESTED IN

[Conversion of spin current into charge current at room temperature: Inverse spin-Hall effect](#)
Applied Physics Letters **88**, 182509 (2006); <https://doi.org/10.1063/1.2199473>

[Spin transfer torque devices utilizing the giant spin Hall effect of tungsten](#)
Applied Physics Letters **101**, 122404 (2012); <https://doi.org/10.1063/1.4753947>

[Inverse spin-Hall effect induced by spin pumping in metallic system](#)
Journal of Applied Physics **109**, 103913 (2011); <https://doi.org/10.1063/1.3587173>

Lock-in Amplifiers
up to 600 MHz



The spin Hall angle and spin diffusion length of Pd measured by spin pumping and microwave photoresistance

X. D. Tao, Z. Feng, B. F. Miao, L. Sun, B. You, D. Wu, J. Du, W. Zhang, and H. F. Ding^{a)}

Department of Physics, National Laboratory of Solid State Microstructures, Nanjing University, 22 Hankou Road, Nanjing 210093, People's Republic of China

(Presented 5 November 2013; received 22 September 2013; accepted 17 October 2013; published online 16 January 2014)

We present the experimental study of the spin Hall angle (SHA) and spin diffusion length of Pd with the spin pumping and microwave photoresistance effects. The Py/Pd bilayer stripes are excited with an out-of-plane microwave magnetic field. The pure spin current is thus pumped and transforms into charge current via the inverse spin Hall effect (ISHE) in Pd layer, yielding an ISHE voltage. The ISHE voltage can be distinguished from the unwanted signal caused by the anisotropic magnetoresistance according to their different symmetries. Together with Pd thickness dependent measurements of in and out-of-plane precessing angles and effective spin mixing conductance, the SHA and spin-diffusion length of Pd are quantified as 0.0056 ± 0.0007 and 7.3 ± 0.7 nm, respectively. © 2014 AIP Publishing LLC. [<http://dx.doi.org/10.1063/1.4862215>]

Spin and charge conversion is one of the essential ingredients of spintronics.¹ Recently, the spin Hall effect (SHE) and its inverse effect, ISHE, have drawn increasing attention as they can achieve the spin and charge conversion in the absence of magnetic material and magnetic field.² The SHE refers to the generation of a spin current transverse to the charge current in a paramagnetic metal or a doped semiconductor.^{3–5} Vice versa, a spin current can give rise to a transverse charge current, i.e., the ISHE. ISHE has also been reported in magnetic material very recently, such as Py.⁶ The efficiency of the spin-charge conversion can be quantified by a single material-specific parameter, i.e., the spin Hall angle (SHA), θ_{SH} . It is defined as the ratio of the spin Hall and charge conductivities.⁷ The SHA can be measured through the nonlocal magneto-transport measurements^{8,9} or the method based on spin pumping due to ferromagnetic resonance (FMR).^{10–12} Because of the complexity of the interface effect, it is typically difficult to estimate the exact amplitude of the injected pure spin current with the first method. While the second method is of more advantage as the above difficulty can be overcome with additional FMR measurements. In real experiments, however, the ISHE signal generated from spin pumping is typically mixed with the unwanted effect related to the anisotropic magnetoresistance (AMR).^{2,10–12} Therefore, the separation of the ISHE signal from the other effect is crucial for the SHA quantification based on spin pumping. In addition, the measured ISHE voltage depends on the SHA, the amplitude of the injected pure spin current as well as the spin diffusion length λ_{sd} . Thus, the correct measurements of the amplitude of the injected pure spin current and the spin diffusion length are also very essential.

In our previous paper, we have developed a method to quantify the spin Hall angle of Pt from spin pumping and

microwave photoresistance measurements.¹² In this method, the AMR related effect can be excluded under a designed geometry due to its different symmetries with the ISHE. The effective spin mixing conductance and precessing angles can be further determined from enhanced Gilbert damping and microwave photoresistance measurements, respectively. Up to now, the SHE and ISHE have been mainly discussed in 5d metals, such as Pt,^{10–13} Au,^{2,14} and Ta.¹⁵ Pd, a 4d transition metal, which also has strong spin-orbit coupling and large spin Hall conductivity,¹⁶ however, is less addressed. Therefore, it is important to quantify the spin Hall angle and the spin diffusion length of Pd.

Py/Pd bilayers are deposited on GaAs substrate by *dc* magnetron sputtering at room temperature, and patterned into stripes with lateral dimension of $2.5 \text{ mm} \times 20 \text{ }\mu\text{m}$. The samples are placed in the slots between the signal and ground line of a coplanar waveguide (CPW) [Fig. 1(a)]. In this configuration, the *rf* magnetic field is perpendicular to the sample plane. We fix the thickness of Py at 16 nm, and study the ISHE of Pd by varying Pd thickness from 3 to 40 nm.

According to the basic theory of spin pumping,^{11,17} the precessing magnetization inside the ferromagnet (Py) pumps a net *dc* pure spin current into its adjacent nonmagnetic (Pd) layer. The magnetic field (*H*) dependence of the injected spin current at the interface can be written as $j_s^0(H) = \frac{\hbar}{2} g_{eff}^{\uparrow\downarrow} f \alpha_1 \beta_1 \Delta H^2 / ((H - H_0)^2 + \Delta H^2)$, where H_0 is the resonance magnetic field, ΔH is the half-width of the FMR linewidth, and α_1 and β_1 are the maximum amplitudes of the in- and out-of-plane precessing angles of the magnetization at resonance. $g_{eff}^{\uparrow\downarrow}$ is the effective spin-mixing conductance and it can be determined experimentally. After being injected into Pd layer, the spin current gives rise to a transverse charge current flowing within the NM layer (with length *L*, width *w*, and resistance R_N). Thus, a *dc* voltage V_{ISHE}^{SP} can be measured along the x-direction [Fig. 1(b)].

^{a)}Author to whom correspondence should be addressed. Electronic mail: hfding@nju.edu.cn.

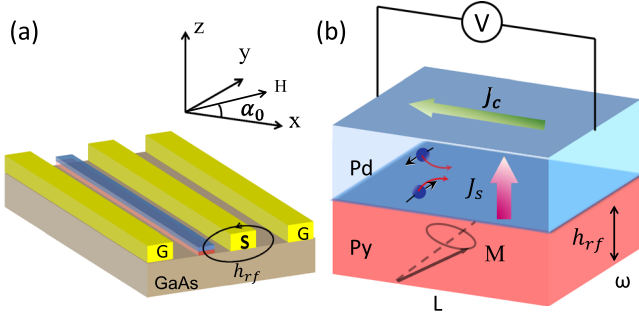


FIG. 1. (a) Experimental geometry for the ISHE measurements via spin pumping: the Py/Pd bilayer stripes are integrated into the slots of a CPW and with an out-of-plane microwave magnetic field. (b) Schematic illustration of the ISHE induced by spin pumping.

Assuming, the SHA θ_{SH} and spin diffusion length λ_{sd} are constants, the integrated ISHE voltage can be calculated as

$$V_{ISHE}^{SP} = \theta_{SH} \lambda_{sd} \tanh\left(\frac{t_N}{2\lambda_{sd}}\right) g_{eff}^{\uparrow\downarrow} R_N f e w \alpha_1 \beta_1 \times \sin \alpha_0 \frac{\Delta H^2}{(H - H_0)^2 + \Delta H^2}, \quad (1)$$

where α_0 is the angle between H and the x -axis, as shown in Fig. 1(a). Meanwhile, the microwave also generates an induction current $I_1 \cos(\omega t)$ and the precessing magnetization results an oscillating resistance $R(t) = R_0 - R_A \sin^2[\alpha_0 + \alpha_1(\omega t)]$ due to the AMR effect. The combination of both gives rise to an additional voltage in the FM stripe, V_{AMR} and it is proportional to $\sin 2\alpha_0$.^{18,19} As discussed above, V_{ISHE}^{SP} and V_{AMR} have different angular dependences with respect to α_0 . This provides a unique opportunity to disentangle V_{ISHE}^{SP} from the mixed signal. In our measurements, we choose two specific geometries, i.e., $\alpha_0 = 90^\circ$ and 270° , where V_{AMR} vanishes but the pure V_{ISHE}^{SP} has its maximum amplitude. Fig. 2(a) shows the typical results of the measured dc voltage as a function of H for $\alpha_0 = 90^\circ$ (black square) and $\alpha_0 = 270^\circ$ (red circle) with the same microwave power input. Both curves exhibit almost a perfect Lorentzian shape, and have opposite sign with respect to each other. They, however, have slightly different amplitudes. This seeming contradiction with the symmetry analysis is due to different spin current injection efficiencies for these two configurations even under the same microwave input power.¹² As shown in Eq. (1), the injected pure spin current is proportional to the product of in- and out-of-plane precessing angles, i.e., $\alpha_1 \beta_1$. These two precessing angles can be determined through the microwave photoresistance measurements.¹⁸ Our measured results show that the precessing angles are $\alpha_1 = 1.41^\circ$, $\beta_1 = 0.41^\circ$ for $\alpha_0 = 90^\circ$ and $\alpha_1 = 1.32^\circ$, $\beta_1 = 0.38^\circ$ for $\alpha_0 = 270^\circ$ for the sample Py(16 nm)/Pd(15 nm) in 8 GHz. They are indeed different for these two configurations. Remarkably but not suprisingly, the normalized voltage $V_{ISHE}^{SP}/\alpha_1 \beta_1$ for $\alpha_0 = 90^\circ$ and 270° falls into an identical curve, evidencing its pure spin pumping origin [Fig. 2(b)]. The inset of Fig. 2(b) shows the Pd thickness dependence of the precessing angles α_1 and β_1 under $\alpha_0 = 90^\circ$ and 270° , respectively. In most cases, the precessing angles for $\alpha_0 = 90^\circ$ is slightly larger than those of 270° . We note that, in our measurements, all the data were obtained with the same input microwave power. But we can

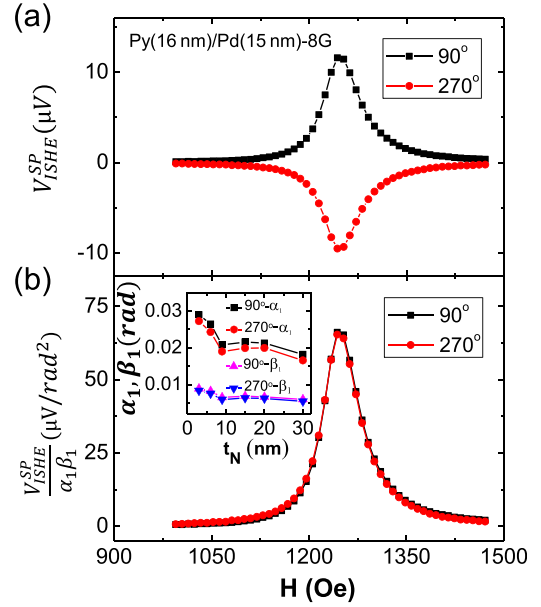


FIG. 2. (a) Field dependence of dc voltage V_{ISHE}^{SP} ($f=8$ GHz) of Py(16 nm)/Pd(15 nm) at $\alpha_0 = 90^\circ$ (black square) and $\alpha_0 = 270^\circ$ (red circle). (b) Normalized inverse spin Hall voltage induced by spin pumping corresponding to Fig. 2(a). The inset shows the thickness dependence of precessing angles for $\alpha_0 = 90^\circ$ and $\alpha_0 = 270^\circ$, respectively.

find that the precessing angles change as function of the Pd thickness. Generally, they become smaller when the Pd thickness increases. This is expected as the screening effect increases with the Pd thickness. The variation can be as large as $\sim 50\%$ from 3 to 30 nm. Thus, we argue that it is very important to measure the precessing angles for each individual sample since the pumped spin current is proportional to the product of in and out-of-plan precessing angles. As we discussed above, V_{AMR} signal has the symmetry of $V_{AMR}(\alpha_0) = V_{AMR}(\alpha_0 + 180^\circ)$, we therefore further redefine a normalized ISHE: $\tilde{V}_{ISHE}^{SP} = (V_{ISHE}^{SP}/\alpha_1 \beta_1|_{90^\circ} - V_{ISHE}^{SP}/\alpha_1 \beta_1|_{270^\circ})/2$ to minimize the residual AMR effect caused by the small experimental misalignment. This also provides a better platform to compare ISHE characteristics of each individual sample since the values are normalized to real microwave power acting on the Py stripes.

As shown in Eq. (1), the spin pumping voltage also depends on the effective spin-mixing conductance $g_{eff}^{\uparrow\downarrow} = 4\pi M_s t_{Py} \alpha_{sp} / g \mu_B$. Where t_{Py} and t_N are the thicknesses of FM and NM layers, M_s is the saturated magnetization of permalloy, α_{sp} is the enhanced Gilbert damping factor due to the loss of spin moment during spin pumping.²⁰ The damping factor can be obtained from the linear fit of the frequency-dependent FMR half linewidth ΔH through $\Delta H = \Delta H_0 + 2\pi \alpha f / \gamma$. The obtained $g_{eff}^{\uparrow\downarrow}$ increases with the increase of Pd thickness and saturates at about 12 nm [Fig. 3(a)], which is in good agreement with the results of Foros *et al.*²⁰ and Shaw *et al.*²¹

As discussed above, in order to obtain the spin Hall angle θ_{SH} of Pd, one needs to perform the Pd thickness dependent measurements as it entangles with the spin diffusion length λ_{sd} in the ISHE voltage. By putting all the parameters that can be measured experimentally to the left side of Eq. (1), we can acquire

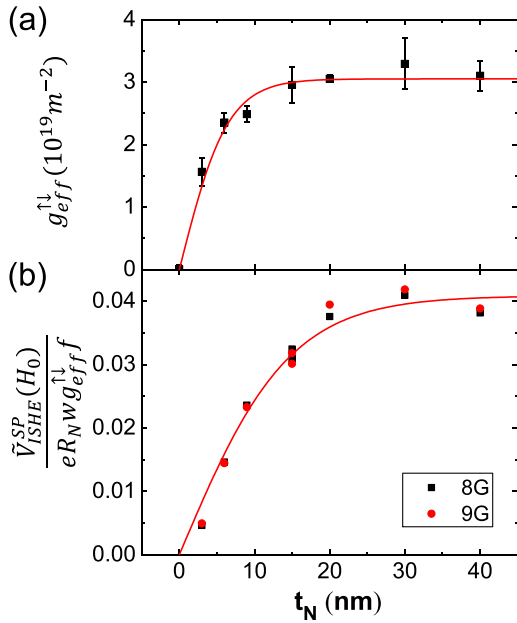


FIG. 3. (a) Pd thickness-dependent g_{eff}^{\downarrow} for Py/Pd (t_N), which reaches saturation at about 12 nm. (b) Experimental determined Pd thickness-dependent $\tilde{V}_{ISHE}^{SP}(H_0)/eR_{NW}g_{eff}^{\downarrow}$ at $f=8$ GHz (black square) and $f=9$ GHz (red circle). The line is the fitted curve according to Eq. (2).

$$\frac{\tilde{V}_{ISHE}^{SP}(H_0)}{eR_{NW}g_{eff}^{\downarrow}} = \theta_{SH}\lambda_{sd} \tanh\left(\frac{t_N}{2\lambda_{sd}}\right). \quad (2)$$

Thus, θ_{SH} and λ_{sd} can be obtained simultaneously through fitting the Pd thickness-dependent measurements. Fig. 3(b) shows the experimental results for $\tilde{V}_{ISHE}^{SP}(H_0)/eR_{NW}g_{eff}^{\downarrow}$ with different Pd thicknesses. To check the reliability of the data, we repeated the measurements for 15 nm thickness as shown in Fig. 3(b). The almost identical values evidence the excellent reproducibility of the data. The small difference in the data obtained with 8 GHz and 9 GHz excitation strongly supports the frequency independence of the SHA, which is expected since what we measured is essentially the *dc* component of ISHE.²² The experimental data show excellent agreement with the fitting utilizing Eq. (2), suggesting the assumption of constant spin Hall angle and spin diffusion length in Eq. (1) is valid within the film thickness range we studied. The fitting simultaneously yields both the spin Hall angle and the spin diffusion length to be $\theta_{SH} = 0.0056 \pm 0.0007$ and $\lambda_{sd} = 7.3 \pm 0.7$ nm, respectively. The obtained SHA and spin diffusion length are in good agreement with Mosendz *et al.*,¹⁰ in which they distangled V_{AMR} and V_{ISHE}^{SP} by assuming that V_{AMR} has only asymmetric component in their particular geometry.

In summary, in combination with the spin pumping and microwave photoresistance measurements, we quantified the

spin Hall angle and the spin diffusion length of Pd using an out-of-plane microwave magnetic field excitation. We demonstrate that one can disentangle the ISHE signal from the unwanted AMR effect with the designed geometries. Through the microwave photoresistance measurements, we found the precessing angles depend on the Pd thickness and the detailed geometry even with the same input microwave power. As the injected spin current is proportional to the product of the in and out-of-plane precessing angles, it is important to measure the precessing angles for each individual sample. The combination of Pd thickness dependent measurements of the ISHE voltage, effective spin mixing conductance and precessing angles yield $\theta_{SH} = 0.0056 \pm 0.0007$ and $\lambda_{sd} = 7.3 \pm 0.7$ nm for Pd.

This work was supported by the State Key Program for Basic Research of China (Grant No. 2010CB923401), NSFC (Grants Nos. 11023002, 11174131, and 11374145).

- ¹S. D. Bader and S. S. P. Parkin, *Annu. Rev. Condens. Matter Phys.* **1**, 71 (2010).
- ²O. Mosendz, J. E. Pearson, F. Y. Fradin, G. E. W. Bauer, S. D. Bader, and A. Hoffmann, *Phys. Rev. Lett.* **104**, 046601 (2010).
- ³J. E. Hirsch, *Phys. Rev. Lett.* **83**, 1834 (1999).
- ⁴S. Zhang, *Phys. Rev. Lett.* **85**, 393 (2000).
- ⁵M. I. Dyakonov and V. I. Perel, *Phys. Lett. A* **35**, 459 (1971).
- ⁶B. F. Miao, S. Y. Huang, D. Qu, and C. L. Chien, *Phys. Rev. Lett.* **111**, 066602 (2013).
- ⁷M. I. Dyakonov and A. V. Khaetskii, in *Spin Physics in Semiconductors*, edited by M. I. Dyakonov (Springer, New York, 2008), p. 212.
- ⁸S. O. Valenzuela and M. Tinkham, *Nature* **442**, 176 (2006).
- ⁹G. Mihajlovic, J. E. Pearson, M. A. Garcia, S. D. Bader, and A. Hoffmann, *Phys. Rev. Lett.* **103**, 166601 (2009).
- ¹⁰O. Mosendz, V. Vlamincik, J. E. Pearson, F. Y. Fradin, G. E. W. Bauer, S. D. Bader, and A. Hoffmann, *Phys. Rev. B* **82**, 214403 (2010).
- ¹¹A. Azevedo, L. H. Vilela-Leão, R. L. Rodríguez-Suárez, A. F. Lacerda Santos, and S. M. Rezende, *Phys. Rev. B* **83**, 144402 (2011).
- ¹²Z. Feng, J. Hu, L. Sun, B. You, D. Wu, J. Du, W. Zhang, A. Hu, Y. Yang, D. M. Tang, B. S. Zhang, and H. F. Ding, *Phys. Rev. B* **85**, 214423 (2012).
- ¹³E. Saitoh, M. Ueda, H. Miyajima, and G. Tatara, *Appl. Phys. Lett.* **88**, 182509 (2006).
- ¹⁴T. Seki, Y. Hasegawa, S. Mitani, S. Takahashi, H. Imamura, S. Maekawa, J. Nitta, and K. Takahashi, *Nature Mater.* **7**, 125 (2008).
- ¹⁵L. Liu, C.-F. Pai, Y. Li, H. W. Tseng, D. C. Ralph, and R. A. Buhrman, *Science* **336**, 555 (2012).
- ¹⁶G. Y. Guo, *J. Appl. Phys.* **105**, 07C701 (2009).
- ¹⁷Y. Tserkovnyak, A. Brataas, and G. E. W. Bauer, *Phys. Rev. B* **66**, 224403 (2002).
- ¹⁸N. Mecking, Y. S. Gui, and C. M. Hu, *Phys. Rev. B* **76**, 224430 (2007).
- ¹⁹L. Bai, Z. Feng, P. Hyde, H. F. Ding, and C. M. Hu, *Appl. Phys. Lett.* **102**, 242402 (2013).
- ²⁰J. Foros, G. Woltersdorf, B. Heinrich, and A. Brataas, *J. Appl. Phys.* **97**, 10A714 (2005).
- ²¹J. M. Shaw, H. T. Nembach, and T. J. Silva, *Phys. Rev. B* **85**, 054412 (2012).
- ²²H. Jiao and G. E. W. Bauer, *Phys. Rev. Lett.* **110**, 217602 (2013).